Materials Research Proceedings **26** (2023) 127-132 https://doi.org/10.21741/9781644902431-21

R-Funicularity of shells and effective eccentricity: Influence of tensile strength

Gloria Rita Argento[1,a *], Stefano Gabriele[1,b] and Valerio Varano[1,c]

[1] Department of Architecture, Roma Tre University, Rome, Italy

[a]gloriarita.argento@uniroma3.it, [b]stefano.gabriele@uniroma3.it, [c]valerio.varano@uniroma3.it

Keywords: R-Funicularity, Generalized Eccentricity, Effective Eccentricity, Tensile Strength

Abstract. The concept of Relaxed Funicularity (R-Funicularity) has been introduced in [2] to deal with the difficulties of designing a shell with a funicular behavior. The R-Funicularity has been defined by using a parameter called generalized eccentricity: a shell is said to be R-Funicular if the generalized eccentricity belongs to an admissibility domain defined in terms of membrane forces N and bending moments M. Here we define an $N-M$ admissibility domain that includes the shell tensile limit force N_t, not previously taken into account. The proposed domain is well described by a new parameter, the effective eccentricity, and is used to control the tensile stresses occurring on shells designed to be R-Funicular and to work under compression.

Introduction

Shells with a funicular shape with respect to a given load are ideally able to bear it without introducing bending. They are an example of mechanical efficiency and subject of a fruitful research [1]. A funicular behavior is difficult to reach due to shell's bending stiffness, boundary conditions or multiple load cases. For this reason, an extension of the funicularity concept has been proposed defining the Relaxed Funicularity (R-Funicularity). A parameter called generalized eccentricity, i.e. the ratio between the generalized bending moments M and the generalized membrane forces N, has been used for this purpose: a shell is R-Funicular if the generalized eccentricity belongs to an admissibility domain [2]. The R-Funicularity has been used to study the modal and dynamic behavior of shells [3]. The velaroidal shells, example of funicular shells [4], have been studied by estimating their R-Funicularity [5,6]. Moreover, the R-Funicularity has been used to assess how the funicularity of timber gridshells is affected by the laths orientation [7]. A shells' shape optimization process aimed to minimize the generalized eccentricity extrema has been developed in [8]. A similar shape optimization process for 1D structures has been proposed in [9].

Here, we introduce an $N-M$ admissibility domain that includes the tensile limit force N_t related to the shell's material and thickness. The proposed domain is well described by the effective eccentricity, a new parameter that will be introduced by means of three main steps. First, the admissibility domain is shifted towards the right to include the tensile strength while showing that the generalized eccentricity is not a good parameter for spanning the new domain. Then, the effective eccentricity is introduced as a change of parameter to left shifting the ellipses. Finally, the mechanical meaning of the effective eccentricity is illustrated.

Generalized Eccentricity and R-Funicularity

Here, we briefly describe the concept of Relaxed Funicularity based on the generalized eccentricity; a complete discussion can be found in [2].

Let us consider a point P belonging to the surface S, endowed with its orthonormal basis $\boldsymbol{a}_1, \boldsymbol{a}_2, \boldsymbol{a}_3$, and a generic direction $\boldsymbol{u} = (\cos\theta, \sin\theta)$ (Fig. 1, Left). The membrane force $N(\theta)$ acting along $\boldsymbol{u}$ and the bending moment $M(\theta)$ acting in the plane $(\boldsymbol{u}, \boldsymbol{a}_3)$ are defined as follows:

Materials Research Proceedings **26** (2023) 127-132 https://doi.org/10.21741/9781644902431-21

$$N(\theta) = \boldsymbol{u}^T \boldsymbol{N} \boldsymbol{u}, M(\theta) = \boldsymbol{u}^T \boldsymbol{M} \boldsymbol{u}, \quad (1a, b)$$

where $\boldsymbol{N}$ and $\boldsymbol{M}$ are the local tensors:

$$\boldsymbol{N} = \begin{pmatrix} N_{11} & N_{12} \\ N_{12} & N_{22} \end{pmatrix}, \ \boldsymbol{M} = \begin{pmatrix} M_{11} & M_{12} \\ M_{12} & M_{22} \end{pmatrix}. \quad (2a, b)$$

The generalized eccentricity is defined as the following ratio:

$$e(\theta) = \frac{M(\theta)}{N(\theta)}. \quad (3)$$

Setting $\alpha = 2\theta$, the following explicit form for Eq. 1a, b has been obtained (Fig. 1, Right):

$$N(\alpha) = \bar{N} + \hat{N}\cos\alpha + N_{12}\sin\alpha, \ M(\alpha) = \bar{M} + \hat{M}\cos\alpha + M_{12}\sin\alpha, \quad (4a, b)$$

where $\bar{N} = \frac{N_{11}+N_{22}}{2}$, $\hat{N} = \frac{N_{11}-N_{22}}{2}$, $\bar{M} = \frac{M_{11}+M_{22}}{2}$, $\hat{M} = \frac{M_{11}-M_{22}}{2}$. Then, the generalized eccentricity is reparametrized:

$$e(\alpha) = \frac{M(\alpha)}{N(\alpha)}. \quad (5)$$

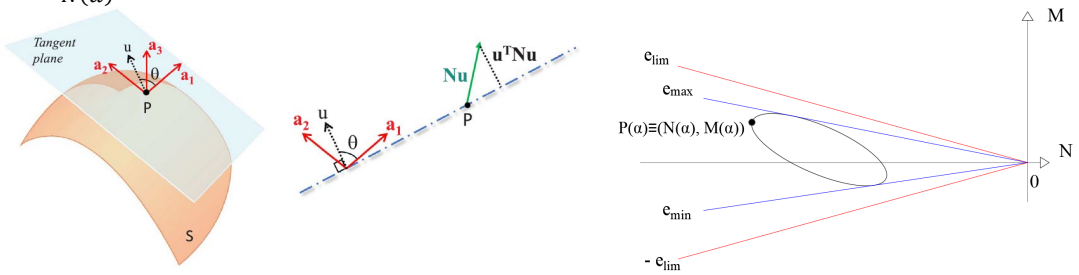

Figure 1 – Left: local basis and projection of internal forces [2]. Right: ellipse of eccentricity or RF ellipse. e_{max} and e_{min} are the slope of the upper and lower blue lines respectively; e_{lim} and $-e_{lim}$ are the slope of the red lines.

It is well known that a 2D structure is funicular if $M(\alpha) = 0 \ \forall \ \alpha$ in each point of the surface. The actual behaviour exhibited by shells with non negligible thickness shows that the nullity of bending moments is an ideal that doesn't verify. The aim of R-Funicularity is to define a criterium to consider a structure funicular in a relaxed manner when $e(\alpha)$ belongs to an admissibility range $[-e_{lim}, e_{lim}]$, where $e_{lim} = \lambda h$, being h the shell thickness and $\lambda \in [0, 1/2]$ an admissibility coefficient. Thus, the Relaxed Funicularity (RF) is defined as follow: "a shell is R-Funicular if, $e(\alpha) \in [-e_{lim}, \ e_{lim}] \ \forall \ \alpha \in [0, \ 2\pi]$, for each point of the surface"(Fig. 1, Right).

In practice the problem of the R-Funicularity is that of verifying:

$$\left[min\left(e(\alpha)\right), \ max\left(e(\alpha)\right)\right] \subset [-e_{lim}, \ e_{lim}]. \quad (6)$$

Writing e as the Rayleigh quotient: $e(\theta) = \frac{\boldsymbol{u^T M u}}{\boldsymbol{u^T N u}}$, the maximum and minimum eccentricities (e_{max}, e_{min}) are found by solving the eigenvalue problem in Eq. 7.

$$(\boldsymbol{M} - e\boldsymbol{N})\,\boldsymbol{u} = 0. \tag{7}$$

The solution of Eq. 7 depends on the algebraic conditioning of $\boldsymbol{M}$ and $\boldsymbol{N}$ and has been discussed in [2]. The local extrema e_{max} and e_{min} of Eq. 7 have been calculated in the equation (17) of [2]. The global extrema of the eccentricities can be finally evaluated as follows:

$$min\big(e(\alpha)\big), max\big(e(\alpha)\big) = \begin{cases} -\infty, +\infty & if\ \det(\boldsymbol{N}) < 0 \\ e_{min}, e_{max} & if\ \det(\boldsymbol{N}) \geq 0 \end{cases}. \tag{8}$$

How to include tensile strength in the analysis

Let us consider a brittle material with a small tensile strength σ_t. This corresponds, in terms of the shell forces to the tensile limit force:

$$N_t = h\,\sigma_t. \tag{9}$$

A simple way to include tensile strength in the admissibility domain is to consider a Mohr-Coulomb like criterion in the plane N, M, by shifting the vertex of the cone from 0 to the positive value N_t. In this way the criterion becomes:

$$|M(\alpha)| \leq -\lambda h\,(N - N_t) = -\lambda h\,N + \lambda h N_t = -\lambda h\,N + M_t. \tag{10}$$

Where the flexural strength $M_t = \lambda h^2\,\sigma_t$ takes over the same role of the cohesion in the Mohr-Coulomb criterion (Fig. 2). The role of the quantity $(N - N_t)$, named effective normal force N_e, arises in Eq. 10.

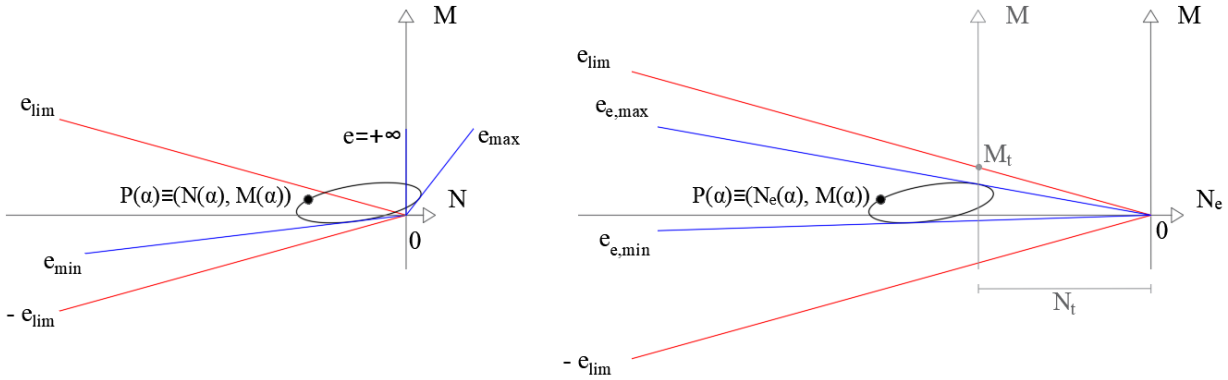

Figure 2 – Ellipse of eccentricities. The slopes of the blue lines and those of the red lines are, respectively, the eccentricity extrema and the eccentricity limits. Left: Eccentricity admissibility domain when no tensile strength is considered. Right: Eccentricity admissibility domain when the tensile limit force N_t is taken into account.

Effective Eccentricity as a change of parameter

In order to properly describe the admissibility domain, we perform a change of parameter, by plotting the ellipse of eccentricity in the plane $(N_e, M) \in \mathbb{R}^2$.

This is done by means of the following substitution:

$$\boldsymbol{N}_e = \boldsymbol{N} - N_t\boldsymbol{I}. \tag{11}$$

Consequently, the expression of the effective normal force in direction $\boldsymbol{u}$ can be calculated as:

$$N_e(\alpha) = \boldsymbol{u}^T\boldsymbol{N_e}\boldsymbol{u} = \boldsymbol{u}^T(\boldsymbol{N} - N_t\boldsymbol{I})\boldsymbol{u} = \boldsymbol{u}^T\boldsymbol{N}\boldsymbol{u} - N_t\boldsymbol{u}^T\boldsymbol{u} = N(\alpha) - N_t. \tag{12}$$

Materials Research Proceedings **26** (2023) 127-132 https://doi.org/10.21741/9781644902431-21

After this change of parameter the ellipse of eccentricity is shifted toward the left and the admissibility domain passes through the origin of the plane (N_e, M). In this way the lines starting from the origin span the admissibility domain. The slope of those that are tangent to the ellipse represent a new descriptor, named *effective eccentricity*:

$$e_e(\alpha) = \frac{M(\alpha)}{N_e(\alpha)} = \frac{M(\alpha)}{N(\alpha)-N_t} = \frac{N(\alpha)}{N_e(\alpha)} e(\alpha). \tag{13}$$

It is worth to notice that $|N_e| > |N|$, being $N < 0$ and $N_t > 0$; thus $e_e(\alpha)$ is proportional to $e(\alpha)$ with the ratio N/N_e and decreases as N_t increases.

Following the definition of the effective eccentricity $e_e(\alpha)$, then the problem of the R-Funicularity becomes to verify:

$$\left[min\left(e_e(\alpha)\right),\ max\left(e_e(\alpha)\right)\right] \subset [-e_{lim}, e_{lim}]. \tag{14}$$

The mechanical meaning of the effective eccentricity is depicted in Fig. 3.

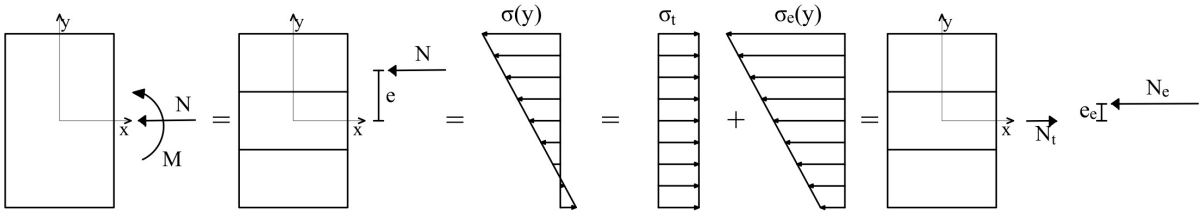

Figure 3 – Graphical representation of the mechanical meaning of the effective eccentricity.

With reference to Fig. 3, the left section is subject to N and M. These are substituted by the eccentric force N, located at distance e from the centre of the section. The stress distribution $\sigma(y)$ due to the eccentric force N goes from compression (top) to tension (bottom) and can be expressed as the sum of the uniform tensile stress distribution σ_t and a trapezoidal one of compression. This is equivalent to the stress state occurring on a section subject to N_t and N_e, the latter being an eccentric force located at distance e_e from the centre of the section. Thus, when the effective eccentricity e_e belongs to the middle-third, the tensile strength is not exceeded.

Example

The effective eccentricity has been evaluated with reference to a well-known funicular surface [4], the parabolic velaroidal surface, described by the following equation:

$$z = f(x,y) = c\left(\frac{x^2}{a^2} - 1\right)\left(\frac{y^2}{b^2} - 1\right), \tag{15}$$

where a and b are the measures of the spans and c is the rise of the surface (Fig. 4).

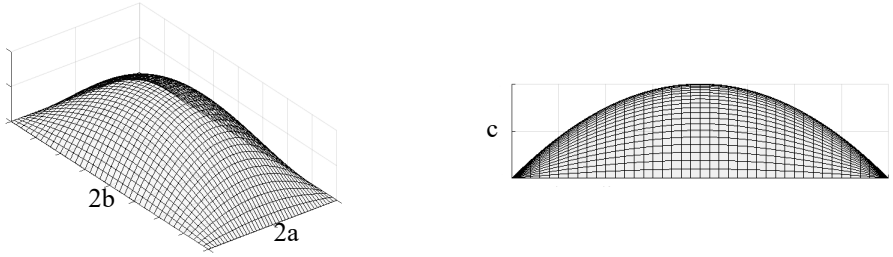

Figure 4 – A parabolic velaroidal surface.

Materials Research Proceedings **26** (2023) 127-132 https://doi.org/10.21741/9781644902431-21

Here we have set $a = b = 10\ m$, $c = 5\ m$; the shell material is concrete with a weight per unit volume $w = 25\ kN/m^3$ and a tensile strength $\sigma_t = 2\ MPa$, the shell thickness is $h = 0.1\ m$ and the admissibility coefficient $\lambda = 1/6$. A finite element model of the shell structure clamped along the entire perimeter has been built, a shell-thin element formulation has been used. Then, a linear static analysis of the shell subject to self-weight has been performed and the results have been used to evaluate the eccentricities and the effective eccentricities (Fig. 5).

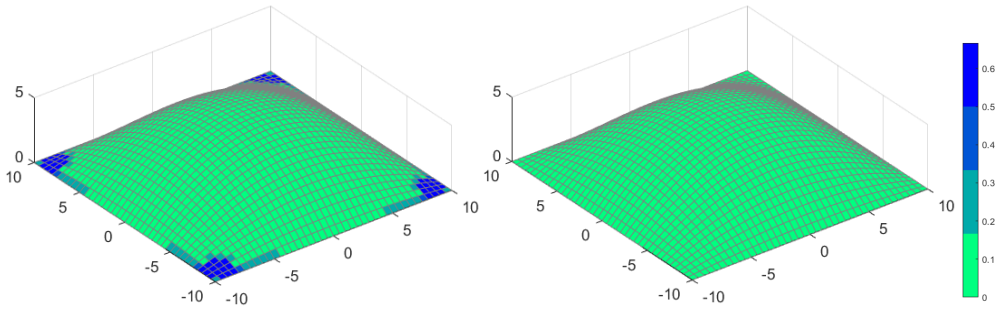

Figure 5 – Left: eccentricity distribution. Right: effective eccentricity distribution.

In Fig. 5, the colormap of the left graph represents the values of $e_{M,i} = max\ (|e_{max,i}|, |e_{min,i}|)$ that increases going from green to blue, the latter meaning that the eccentricity is $> h/2$, i.e. the resultant force N acts out of the cross section. The shell is R-Funicular in the light green areas. The effective eccentricities $e_{e_{M,i}} = max\ (|e_{e_{max,i}}|, |e_{e_{min,i}}|)$, are hence pictured with the colormap of the right graph, with the same color scale of the left one. In this case the effective eccentricity is everywhere included in the admissibility domain.

By exploiting the symmetry of the studied surface, the ellipse of eccentricities has been evaluated for the shell elements shown in Fig. 6.

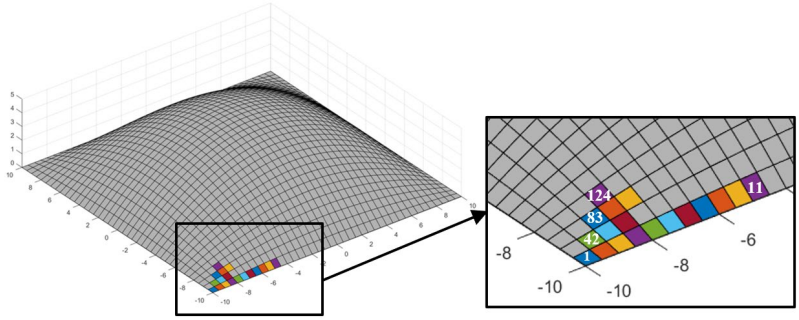

Figure 6 – Non R-Funicular shell elements that turn R-Funicular when the tensile strength is considered.

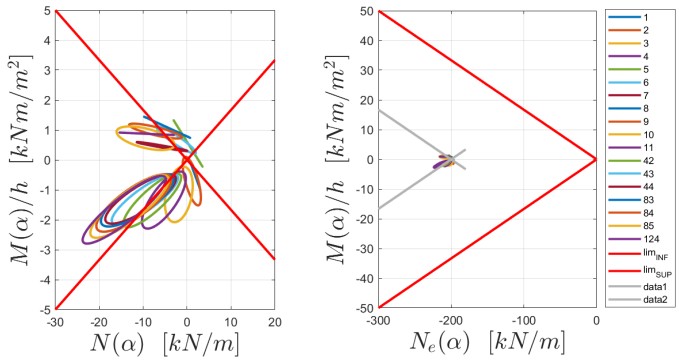

Figure 7 – Left: ellipse of eccentricity of the non R-Funicular shell elements. Right: the shell elements turn R-Funicular when the extended domain is considered.

As shown in Fig. 5 and in Fig. 7, the shell structure, originally non R-Funicular in the areas close to the boundaries, turns R-Funicular when the tensile strength is taken into account.

Conclusions

In this work has been developed the idea of how to formally extend the admissibility domain of shell's R-Funicularity by taking into account the tensile strength of the material. A new parameter called effective eccentricity has been introduced on purpose, in order to consider the left shifting of the R-Funicularity ellipses. The mechanical meaning of the effective eccentricity has been illustrated. The presented numerical example shown as a partially non R-Funicular shell turns fully R-Funicular when the extended domain is used. As a first work in this direction the authors are aware that taking into account the small tensile strength of shells, designed to work in compression, is a tricky task. For this reason, further development of the work will aim to account for the contribution of the prestress exploiting a formulation analogous to that here used.

References

[1] S. Adriaenssens, P. Block, D. Veenendaal, C. Williams, Shell structures for architecture: form finding and optimization, New York: Routledge, 2014. https://doi.org/10.4324/9781315849270

[2] S. Gabriele, V. Varano, G. Tomasello, D. Alfonsi, R-Funicularity of form found shell structures, Eng. Struct. 157 (2018) 157-169. https://doi.org/10.1016/j.engstruct.2017.12.014

[3] G. Tomasello, S. Adriaenssens, S. Gabriele, Dynamic behavior of form-found shell structures according to Modal and Dynamic Funicularity, Eng. Struct. 198 (2019) 109521. https://doi.org/10.1016/j.engstruct.2019.109521

[4] G. S. Ramaswamy, Design and construction of a new shell of double curvature, in: Proceedings of the Symposium on Shell Research, Delft, 1961, North Holland Publishing Co. Amsterdam, pp. 102-115.

[5] S. Gabriele, F. Marmo, V. Varano, About the funicularity of Velaroidal Shells, in: C. Lázaro, K.-U. Bletzinger, E. Oñate (Eds.), Proceedings of the IASS Annual Symposium 2019 - Structural Membranes 2019, Form and Force, Barcellona, Spain, 7-10 October 2019, 2019, pp. 45-52.

[6] F. Marmo , S. Gabriele, V. Varano, S. Adriaenssens, R-Funicularity of Analytical Shells, in: A. Carcaterra, A. Paolone, G. Graziani (Eds), Proceedings of XXIV AIMETA Conference 2019, Lecture Notes in Mechanical Engineering, Springer, 2020, pp. 947-957. https://doi.org/10.1007/978-3-030-41057-5_77

[7] M.L. Regalo, S. Gabriele, G. Salerno, V. Varano, Numerical methods for post-formed timber gridshells: Simulation of the forming process and assessment of R-Funicularity, Eng. Struct. 206 (2020) 110119. https://doi.org/10.1016/j.engstruct.2019.110119

[8] G.R. Argento, F. Marmo, V. Varano, S. Gabriele, Shells' shape optimization based on R-Funicularity, in: S. A. Behnejad, G. A. R. Parke, O. A. Samavati (Eds.), Inspiring the Next Generation - Proceedings of the International Conference on Spatial Structures 2020/21 (IASS2020/21-Surrey7), Guildford, UK, 23-27 August 2021, 2021, pp. 2548-2556.

[9] G. R. Argento, S. Gabriele, V. Varano, R-Funicularity for shells' shape optimization, in: C. Fivet, P. D'Acunto, M. Fernández Ruiz, P. O. Ohlbrock (Eds.), Proceedings of the International *fib* Symposium on the Conceptual Design of Structures, Attisholz Areal, Switzerland, 16-18 September 2021, 2021, pp. 503-510. https://doi.org/10.35789/fib.PROC.0055.2021.CDSymp.P062